The low-temperature heat capacity of fullerite C_{60}

M.I. Bagatskii, V.V. Sumarokov, M.S. Barabashko, and A.V. Dolbin

B. Verkin Institute for Low Temperature Physics and Engineering of the National Academy of Sciences of Ukraine
47 Lenin Ave., Kharkov 61103, Ukraine
E-mail: bagatskii@ilt.kharkov.ua

B. Sundqvist

Department of Physics, Umea University, SE-901 87 Umea, Sweden

The heat capacity at constant pressure of fullerite C_{60} has been investigated using an adiabatic calorimeter in a temperature range from 1.2 to 120 K. Our results and literature data have been analyzed in a temperature interval from 0.2 to 300 K. The contributions of the intramolecular and lattice vibrations into the heat capacity of C_{60} have been separated. The contribution of the intramolecular vibration becomes significant above 50 K. Below 2.3 K the experimental temperature dependence of the heat capacity of C_{60} is described by the linear and cubic terms. The limiting Debye temperature at $T \to 0$ K has been estimated ($\Theta_0 = 84.4$ K). In the interval from 1.2 to 30 K the experimental curve of the heat capacity of C_{60} describes the contributions of rotational tunnel levels, translational vibrations (in the Debye model with $\Theta_0 = 84.4$ K), and librations (in the Einstein model with $\Theta_{E,\text{lib}} = 32.5$ K). It is shown that the experimental temperature dependences of heat capacity and thermal expansion are proportional in the region from 5 to 60 K. The contribution of the cooperative processes of orientational disordering becomes appreciable above 180 K. In the high-temperature phase the lattice heat capacity at constant volume is close to 4.5 R, which corresponds to the high-temperature limit of translational vibrations (3 R) and the near-free rotational motion of C_{60} molecules (1.5 R).

Introduction

Since the discovery of the fullerite molecule C_{60} [1], the low-temperature physical properties of fullerite C_{60} have been investigated by various methods: inelastic neutron scattering [2,3], infrared and Raman spectroscopy [4,5], x-ray [3,6,7], neutron [8] and electron [9,10] diffraction, NMR [11], dilatometry [12–15] and calorimetry [16–25]. It has found that fullerite C_{60} is a molecular crystal in which the molecules are bonded by the van der Waals forces and its physical properties are largely determined by the dynamics of the rotational motion of the C_{60} molecules. At $T_c \approx 260$ K fullerite undergoes an orientational phase transition from a high-temperature face-centered cubic (FCC) lattice to a low-temperature simple cubic (SC) one [7,8]. The high-temperature phase has no long-range orientational order and the rotational motion of the molecules is slightly hindered. In the low-temperature phase the centers of gravity of the molecules remain in FCC sites and molecules form four SC sublattices having different orientations of the axes of three-fold symmetry along the body diagonals of the cube (<111> directions). In the orientationally ordered phase by the rotation of the molecules about the <111> axes the molecules can be in six potential wells with global and local minima, which correspond to the pentagonal (p) and hexagonal (h) configurations, respectively. In the p-configuration one of the five-fold axes of the molecule is directed toward the middle of one of the double bonds of the neighboring molecule. In the h-configuration the three-fold axis of the molecule is directed toward the center of the double bond of the neighboring molecule [8,26]. The barrier between the wells is about

2900 K and the energy difference between the minima in the potential wells of the p- and h-configurations is ≈ 120 K. Below T_c the C_{60} molecules either perform orientational vibrations (librations) in the potential wells or execute retarded rotation hopping between the nearest potential wells. The phase transition is cooperative in nature. The molecule concentrations n_p and n_h in the p- and h-configurations are dependent on temperature. In the low-temperature phase $n_p \approx 63\%$ near $T_c \approx 260$ K (see Fig. 10 in [2]). At lowering temperature n_p increase and the frequency of hopping decreases. At the temperature of glass formation T_g (80–90 K) the reorientational motion of the molecules is frozen and fullerite changes to the state of orientational glass with $n_p \approx 83\%$ (see Fig. 10 [2]). This occurs because the energy of the molecules is no longer sufficient to overcome the potential barrier between the p- and h-configurations [2,8,27]. The presence of a high (≈ 2900 K) barrier between the p- and h-configurations places the emphasis on the influence of the temperature prehistory on the physical properties of C_{60} crystals, which entails the hysteretic phenomena in the regions of phase transition.

The heat capacity at constant pressure $C_p(T)$ of C_{60} was investigated by the adiabatic method in Refs. 16, 17 (at a temperature range 11–300 K), [18] (13–300 K), [19] (5–340 K), [20] (6–350 K), [21] (1.2–30 K) and by thermal relaxation method in [22,23] (1.4–20 K), [24] (4–300 K) and [25] (0.2–190 K). In interval from 4 to 160 K the discrepancy between the data in [16–23] is within 25%. The data in [24] are 50–100% over those in [16–23]. Olson *et al.* [25] investigated a solid ~15% C_{70}–C_{60} mixture. Therefore their $C_p(T)$ differs significantly in value and behavior from the results in [16–24]. The systematic discrepancy between both the curves $C_p(T)$ and the T_c — values taken on heating the samples in adiabatic calorimeters [16–21] are due to the variations in the purity [16,17,28] and perfection [20] of the samples. The systematic scatter of the data on the thermodynamic properties of C_{60} is also caused by the influence of the temperature prehistory of the samples and by thermocycling [29–31]. Grivei *et al.* [24] observed a large hysteresis of $C_p(T)$ in the region from 160 to 286 K.

The heat capacity of C_{60} was investigated below 4 K [21–23,25]. Beyermann *et al.* [22,23] performed two series of $C_p(T)$ measurements. In series 2 the samples were pre-annealed in vacuum at 430 K. Above 4 K the data discrepancy between series 1 and 2 was within 16%. At $T < 2$ K the results of series 1 were an order of magnitude higher than in series 2. The distinctions between the $C_p(T)$ data in series 1 [22] and 2 [23] were attributed [23] mainly to the different concentrations of the solvent impurity in the C_{60} samples. In the interval from 4 to 20 K the results of series 2 [23] are systematically 5–12% higher than the data in [21]. As temperature decreases, the data distinctions between [21] and [23] increase and at 1.4 K the C_p in [23] is about five times higher than in [21].

Below 2.2 K [23] and 0.7 K [25] the data are described by the linear and cubic terms, respectively:

$$C_p(T) = A_1 T + A_3 T^3 . \tag{1}$$

According to [23], the linear term in $C_p(T)$ is more sensitive to the solvent impurity. It is determined by the contribution of the tunnel levels in the orientational glass phase of fullerite C_{60} [22,25]. The contribution described by the cubic term is fully dependent on the density of states of acoustic phonons. The limiting Debye temperature $\Theta_0 = 80$ K at $T \to 0$ was estimated using A_3 [25]. Beyermann *et al.* [23] and Nemes *et al.* [32] analyzed the experimental results on $C_p(T)$. By varying four parameters A_1, Θ_0, $\Theta_{E,tr}$ and $\Theta_{E,lib}$ they calculated the contributions of tunnel levels (A_1), acoustic phonons within the Debye model with the temperature Θ_0 and optical translational and librations within the Einstein model with characteristic temperatures $\Theta_{E,tr}$ and $\Theta_{E,lib}$, respectively. They obtained $\Theta_0 = 37$ K [23] and $\Theta_0 = 32$ K [32]. From the analysis of $C_p(T)$ above 50 K $\Theta_0 \approx 50$ K [16,17] and $\Theta_0 \approx 60$ K [33]. Houen *et al.* [34] calculated $\Theta_0 \approx 100$ K from the low-temperature Young modulus of single-crystalline C_{60}. $\Theta_0 \approx 54$ K was derived from the analysis of temperature dependence of the thermal expansion coefficient of polycrystalline C_{60} and its solutions with Ne and Ar [14]. In [7] the ultrasonic velocities of polycrystalline C_{60} were analyzed and extrapolated to low temperatures, which yielded $\Theta_0 \approx 55.4$ K. Shebanovs *et al.* [35] obtained the Debye temperature $\Theta_D(280$ K$) \approx 53.9$ K by analyzing the x-ray diffraction data for single-crystalline C_{60} at 280 K. $\Theta_D(300$ K$) \approx 66$ K was obtained from the ultrasonic velocities measured in a C_{60} single crystal at 300 K [36]. Mikhalchenko [37] analyzed literature data on Θ_0 of fullerite C_{60}. Author [37] calculated $\Theta_0 = 77.12$ K from the harmonic elastic constants c_{ijkl} of a C_{60} single crystal at 0 K.

The large scatter of Θ_0-data is a good motivation to continue low-temperature investigation of the physical properties of fullerite C_{60}. Θ_0 is a constant which characterizes the properties of a crystal, such as heat capacity, electric and thermal conductivities, x-ray spectra intensity, elastic features. Θ_0 is also a characteristic parameter separating the high temperature region ($T \gg \Theta_0$), where the lattice vibrations can be described within the classical theory, and the low-temperature region ($T \ll \Theta_0$), where the quantum mechanical effects become significant [38].

Note that the data on the heat capacity of C_{60} are essential for analyzing the heat capacities of new C_{60}-containing nanomaterials, for example, elementary atomic and molecular gaseous substances that form interstitial solutions in the octahedral voids of fullerite C_{60} [39–41].

Goal of this study was to investigate the low-temperature dynamics of fullerene C_{60} by the calorimetric method.

M.I. Bagatskii, V.V. Sumarokov, M.S. Barabashko, A.V. Dolbin, and B. Sundqvist

Experiment

The heat capacity at constant pressure $C_p(T)$ of fullerite C_{60} was investigated in a temperature interval from 1.2 to 120 K in an adiabatic calorimeter [21]. Two experiments were made. In the first experiment the heat capacity of the sample was measured from 1.2 to 30 K [21]. In the second experiment the sample was first heated to ~ 320 K and held in the dynamic vacuum ($\approx 1 \cdot 10^{-3}$ Torr) for about 48 hours. The calorimeter was cooled through wires without using helium as an heat exchange gas. Then measurements were made in the interval from 1.2 to 120 K. $C_p(T)$ of fullerite C_{60} was obtained by subtracting addenda $C_{ad}(T)$ (the heat capacity of an empty calorimeter with the Apiezon grease) from the total heat capacity of the calorimeter with the sample. $C_{ad}(T)$ was measured in a special experiment.

The sample was a cylinder about 6 mm high and 10 mm in diameter. It was prepared at Umea University (Sweden) by compacting a C_{60} powder under pressure about 1 kbar. The characteristic sizes of the C_{60} crystallites varied within 0.1 to 0.3 mm. The C_{60} purity was 99.99%. The masses of the C_{60} sample and the Apiezon grease were $m_f = (586.48 \pm 0.05)$ mg and $m_A = (0.45 \pm 0.05)$ mg, respectively. The information about the C_{60} sample and the calorimeter is detailed elsewhere [14,21].

The contribution of the sample to the total heat capacity of the calorimeter with the sample was 45% below 2 K, about 70% in the interval from 4 to 20 K, 45% at 30 K and 23% at 120 K. The random experimental error in the specific heat of fullerite C_{60} was ±40% at 1.3 K, ±30% at 2 K, ±5% at 4 K and ±1.5% in the interval from 30 to 120 K.

Results and discussion

The experimental results on the specific heat $C_p(T)$ of fullerite C_{60} and the literature data [16–25] are illustrated in Fig. 1 for the temperature regions 0.2–300 K (a), 0.2–120 K (b) and 0.2–50 K (c) in the lg-lg scale representation. Our results obtained in experiments 1 [21] and 2 coincide. According to [7], the difference $C_p(T)–C_v(T)$ is 0.18 mJ/(g·K) at 120 K, 1.17 mJ/(g·K) at 160 K and 4 mJ/(g·K) at 290 K, which makes about 0.1%, 0.4% and 0.6% of $C_p(T)$, respectively. The difference $C_p(T)–C_v(T)$ is negligible below 160 K.

It is seen that two experimental curves [24,25] are significantly distinct from the others. There is a giant hysteresis in temperature range from 160 to 286 K [24]. The curve $C_p(T)$ measured on heating the calorimeter has a maximum at 286 K and a minimum at 255 K. The curve $C_p(T)$ taken on cooling the calorimeter has two maxima at 157 and 252 K and two minima at 202 and 266 K [24] (see Fig. 1(a)). For our opinion the distinctions between [25] and [16–24] is the effect of the impurity ~15% C_{70} in the sample. Note that above 40 K the contribution of the impurity C_{70} is higher even at low concentrations because the C_{70} molecule has 30 intramolecular frequencies more than the C_{60} molecule.
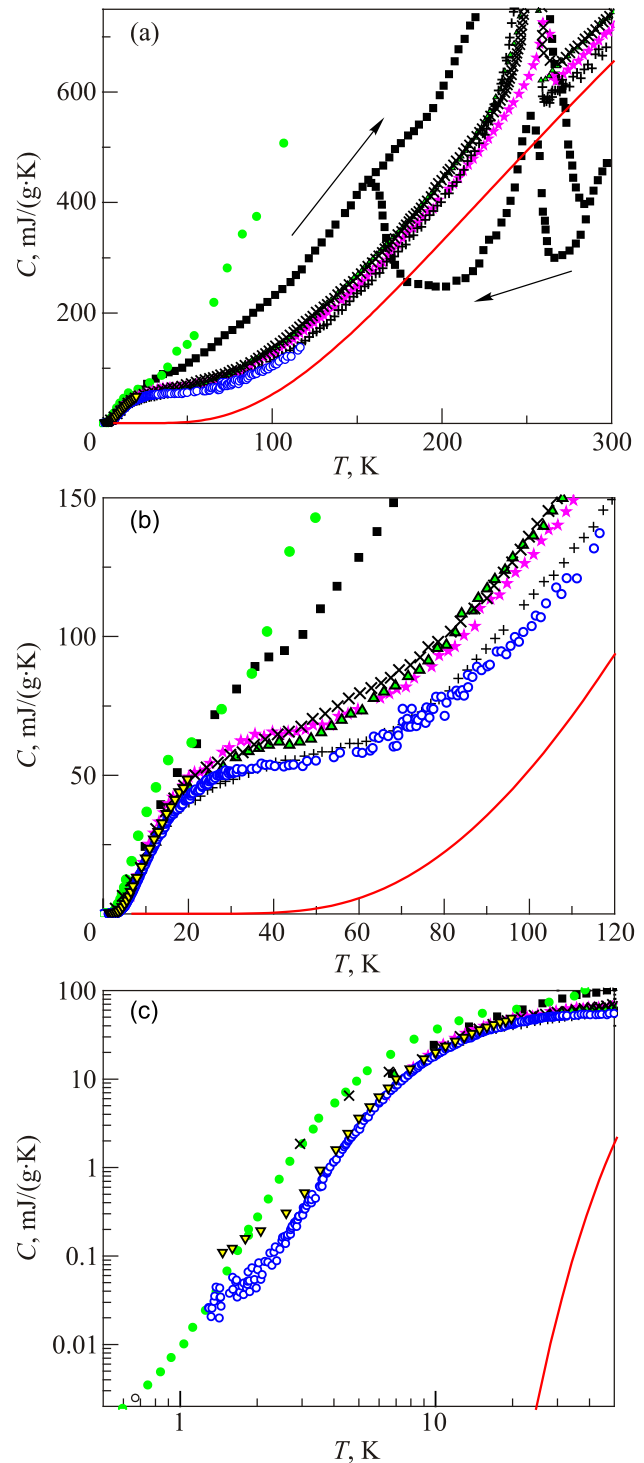

Fig. 1. (Color online) The temperature dependence of the specific heat of C_{60} in temperature range 0.2–300 K (a), 0.2–120 K (b), and 0.2–50 K (c), lg-lg scale. Experimental results: (○) — this work and [21], (+) — [16,17], (Δ) — [18], (×) — [19], (★) — [20], (∇) — [23], (■) — [24], (●) — [25]. The contribution of intramolecular vibrations C_{in} (solid line) to the heat capacity of C_{60} was calculated within the Einstein model using the vibration frequencies of the carbon atoms in the C_{60} molecule [42].

It is seen (Figs. 1(a),(b)) that our results agree well with the data of Atake *et al.* [16,17] (in interval 11–120 K) and Beyermann *et al.* [23] (4–20 K). At $T < 4$ K the distinction between our results and [23] increases. Near 1.5 K the data of [23] are five times higher than our results. Near 1.4 K our C_p values are close to those in [25] (see Fig. 1(c)). In the interval from 8 to 40 K the data of [18–20] are on the average 8% higher than our results. Note that in [16–20] the samples were hermetically sealed in calorimeter vessels, and the sample-calorimeter thermal contact was improved by feeding helium gas to the calorimeter at room temperatures. At this temperature the He atoms can occupy the octahedral voids in the C_{60} crystal [43,44]. Saturation of C_{60} with He takes several hours [44]. The presence of helium in the calorimetric vessels and the samples can lead to higher systematic errors. In our experiments the calorimetric cell was cooled through wires, without using helium as an heat exchange gas. Above 40 K the distinctions in the data of [16–25] increase. This may be caused by the presence of the C_{70} impurity (this work, Fig. 1(a) and [28]) and the solvent (see Fig. 2 in [17]) or disturbance of the equilibrium concentrations n_p and n_h at T_g as well as by helium gas.

The heat capacity of a C_{60} single crystal with a minimum of structural defects was measured in a temperature range from 6 to 350 K by Miyazaki *et al.* [20]. They observed the sharpest maximum in the curve $C_p(T)$ and highest phase transition temperature $T_c = 262.1$ K. It was found that the transition from the orientational glass state to a partially orientationally-ordered phase occurred in a range from 80 to 90 K. The difference between the heat capacities above and below $T_g \approx 84.6$ K is $\Delta C = 3.6$ J/(K mol). The corresponding data in [18] and [19] are $\Delta C = 7$ J/(K·mol) at $T_g \approx 86.8$ K and $\Delta C = 4.5$ J/(K·mol) at $T_g \approx 86$ K, respectively. Below T_g the C_{60} concentrations in the p- and h-configurations are frozen ($n_p \approx 83\%$ [2]). Above T_g the concentration $n_p(T)$ decreases when the temperature rises (see Fig. 10 in [2]). The decrease/increase in n_p is attended with heat absorption/release in the crystal [18,19]. The data on heat capacity [18] and thermal conductivity [45] show that the characteristic time τ of p–h relaxation increases from $\sim 10^3$ s at 90 K to $\sim 10^4$ s at 80 K. Our calorimeter was cooled from 150 to 80 K rather fast (2.5 hours). Therefore the concentration n_p frozen in the sample below 80 K can correspond to the equilibrium concentration at T_f which is higher than T_g. As a result, the heat capacities measured at $T < T_f$ can be lower than in the case of the equilibrium concentration $n_p(T_f)$.

In the region of the glass phase transition the scatter of data is several times higher than at $T < 70$ K and $T > 90$ K (see Fig. 1(b)). This may be attributed to the influence of the temperature prehistory of the sample.

The results obtained and the literature data in temperature range from 0.2 to 300 K [16–25] were analyzed assuming an additive contribution of translational, rotational and intramolecular degrees of freedom to the heat capacity of fullerite. Accoding to the group-theory analysis [46], 174 intramolecular vibrations may be grouped into 46 fundamental modes having characteristic symmetries: A_g (two modes), A_u (one mode), T_{1g} (three modes), T_{1u} (four modes), T_{2u} (five modes), G_g (six modes), H_g (eight modes), H_u (seven modes). The contribution of the intramolecular vibrations $C_{in}(T)$ was calculated using the Einstein model and the data on the vibration frequencies of the carbon atoms in a C_{60} molecule [42]. $C_{in}(T)$ is illustrated in Fig. 1 (solid line). The contribution $C_{in}(T)$ becomes appreciable above 50 K. $C_{in}/C_p \approx 0.5$ at ≈ 100 K (the low-temperature phase) and $C_{in}/C_p > 0.9$ at 270 K (the high-temperature phase) (see Fig. 1(a)). The lattice heat capacity $C_{p,\mathrm{lat}}(T) = C_p(T) - C_{in}(T)$ of fullerite C_{60} is illustrated in Fig. 2. It is seen that $C_{p,\mathrm{lat}}$ is weakly dependent on temperature in the interval from 60 to 150 K. The contribution of the cooperative processes of orientational disordering to the lattice heat capacity of C_{60} is appreciable above 180 K. The peak in the curve $C_{p,\mathrm{lat}}(T)$ at $T_c \approx 260$ K is due to the orientational order-disorder phase transition. At 290 K the $C_{V,\mathrm{lat}}$ value is close to $4.5\,R$ (R is a gas constant). $C_{V,\mathrm{lat}}$ was obtained from the $C_{p,\mathrm{lat}}$ data [20] by subtracting the correction $C_p - C_V \approx 3.0$ J/(K·mol) [7]. This behavior of the heat capacity is consistent with the data in [2,48] which suggest that the rotation of C_{60} molecules is nearly free in the high-temperature phase.

At low temperatures the experimental $C_{p,\mathrm{lat}}(T)$ was analyzed taking into account the contributions of the rotational tunnel levels in orientational glass (C_{tun}), translational (C_D) and libration ($C_{E,\mathrm{lib}}$) vibrational modes. Below 2.3 K our temperature dependence $C_{p,\mathrm{lat}}(T)$ is described by the expression $C_{p,\mathrm{lat}}(T) = 0.01T + 0.00322T^3$ (J/(K·mol)) (see Fig. 3). The linear term describes the contribution of the rotational tunnel levels in orientational C_{60} glass [15,22,23,25,48,49]. This term is sensitive to even low impurity concentrations [23,25]. The impurities randomly distributed in the crystal generate random deformation fields leading to higher stochastization of tunnel levels [50,51].
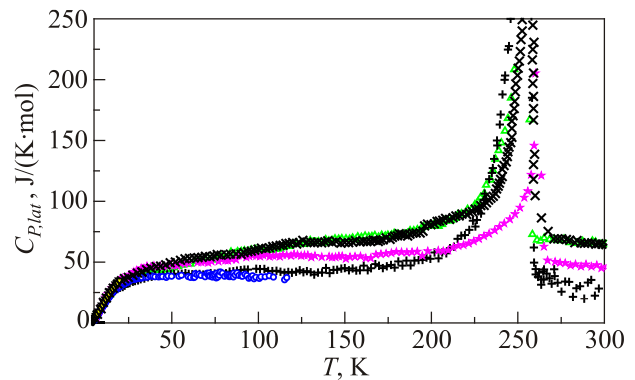

Fig. 2. (Color online) The lattice specific heat $C_{p,\mathrm{lat}}(T) = C_p(T) - C_{in}(T)$ of fullerite C_{60}. Experimental results: ($\circ$) — this work and [21], (+) — [16,17], (Δ) — [18], ($\times$) — [19], ($\star$) — [20], (∇) — [23].
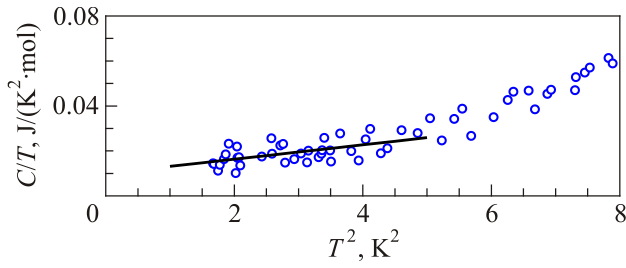
Fig. 3. (Color online) The low-temperature heat capacity of C_{60} in the coordinates C/T vs T^2.

The contribution described by the cubic term ($0.00322T^3$ J/(K·mol) at $T \leq 2.3$ K) is made by acoustic translational vibrations. The limiting Debye temperature at $T \to 0$ K ($\Theta_0 = 84.4$ K) was found using the coefficient at T^3. This value agrees with literature $\Theta_0 = 80$ K obtained for solid solution 15% C_{70} in C_{60} in experiment [25]. Calculation of Debye temperature $\Theta_0 = 77.12$ K was made in [37] by using the harmonic elastic constants c_{ijkl} of a C_{60} single crystal at 0 K. Literature data for Debye temperature are given in the Table 1. This scatter (unusual for solids) in the quantities Θ_0 for the fullerite C_{60} is most likely associated not only with the limitations of the Debye law T^3 (for the C_{60} the corresponding range is extremely narrow, $T \leq 2$ K) but also with the procedures used for calculation.

The contribution C_D of translational vibration modes above 2.3 K was calculated within the Debye model with $\Theta_0 = 84.4$ K. The contribution of libration modes becomes significant above 2.3 K. The contribution of optical libration modes $C_{E,\text{lib}}$ was calculated within the Einstein model. The best fitting between the experimental $C_{p,\text{lat}}$ and calculated $C_{V,\text{lat}}(T) = A_1 T + C_D(\Theta_0, T) + C_{E,\text{lib}}(\Theta_{E,\text{lib}}, T)$ curves in temperature interval from 1.2 to 30 K is observed for $A_1 = 0.01$ J/K^{2}mol, $\Theta_0 = 84.4$ K and $\Theta_{E,\text{lib}} = 32.5$ K. The lattice heat capacities $C_{p,\text{lat}}$ and $C_{V,\text{lat}}$ of C_{60} are com-
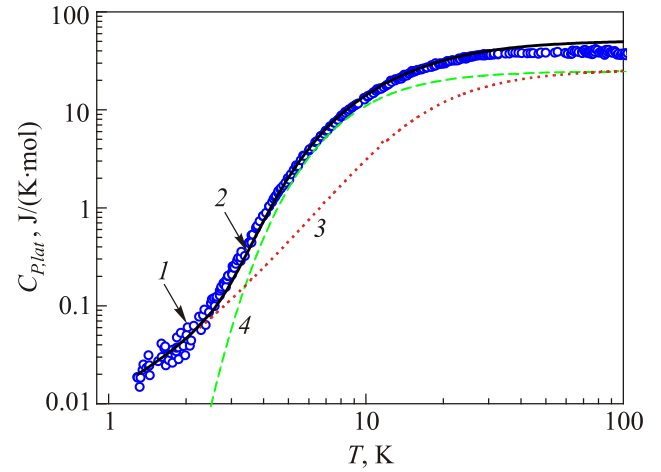

Fig. 4. (Color online) The lattice specific heat $C_{p,\text{lat}}(T) = C_p(T) - C_{\text{in}}(T)$ of C_{60}. Experiment: (*1*) — this work and [21]. Calculation: (*3*) dot line — contribution of tunnel levels and translational vibrations of the lattice ($A_1 T + C_D$), (*4*) dash line — contribution of librations ($C_{E,\text{lib}}$) and (*2*) solid line — the total heat capacity. $C_{V,\text{lat}}(T) = A_1 T + C_D(\Theta_0, T) + C_{E,\text{lib}}(\Theta_{E,\text{lib}}, T)$.

pared in Fig. 4. It is seen that the contributions of the acoustic translational modes and the tunnel levels become dominant below 3 K. The contribution of the librations prevails in the interval from 4 to 20 K.

The densities of states of lattice vibrations (arbitrary units) are illustrated schematically in Fig. 5. The density of states (solid line) was obtained in experiment on inelastic neutron scattering [2]. The dotted and solid lines show the densities of states of the translational modes (Debye model) and optical libration modes (Einstein model) obtained from the analysis of our $C_{p,\text{lat}}(T)$ data. It is seen in Fig. 5 that the first libration (L) maximum in the density of states curve is close to the Einstein temperature $\Theta_{E,\text{lib}} = 32.5$ K.

The behavior of the temperature dependences of the heat capacity $C_p(T)$ and the linear thermal expansion $\alpha(T)$ [14]

Table 1. Debye temperature

Authors	Year	Θ_0, K	Property	Temperature range, K
T. Atake *et al.*	1992	50[*]	Heat capacity	10–300
W.P. Beyermann *et al.* [23]	1992	37	Heat capacity	1.4–20
J.R. Olson *et al.* [25]	1993	80	Heat capacity	0.2–190
N. A. Aksenova *et al.* [7]	1999	55.2[*]	Sound velocity	300
N. P. Kobelev *et al.* [36]	1998	66	Sound velocity	300
A.N. Aleksandrovskii *et al.* [14]	2003	54[**]	Heat expansion	6–12
S. Hoen *et al.* [34]	1992	100	Young's modulus	80–120
M. N. Magomedov *et al.*	2005	58.75	Calculation	0
V. P. Mikhal'chenko [37]	2010	77.12	Calculation from the harmonic elastic constants	0
This paper	2015	84.4	Heat capacity	1–120

C o m m e n t s : [*] ‾ From analysis of high-temperature data

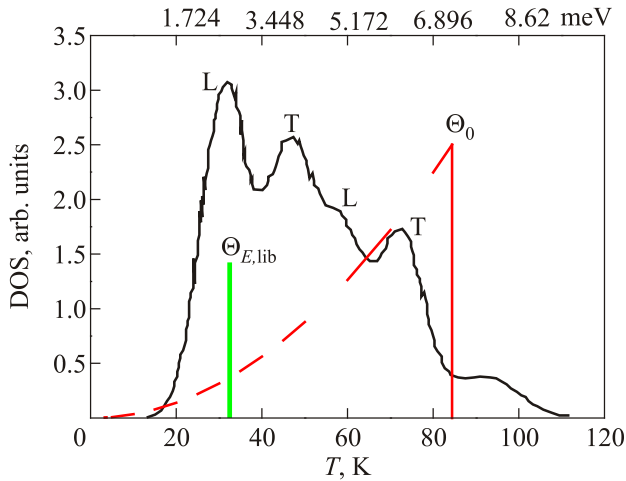[**] ‾ From analysis of temperature dependencies of heat expansion of C_{60} and C_{60} with Ne and Ar admixtures.

Fig. 5. (Color online) The density of states of the lattice vibrations measured on the C_{60} powder by the method of inelastic neutron scattering (solid curve). L and T refer to libration and translation features, respectively The densities of state derived from the analysis of our $C_{p,\text{lat}}(T)$ data are shown for the acoustic mode in the Debye model (straight dashed line), the optical libration mode in the Einstein model (straight solid line).

of C_{60} are compared in Fig. 6 in a range from 1 to 20 K. The linear thermal expansion was scaled along the ordinate axis to match the curves $C_p(T)$ and $\alpha(T)$. The measurements of $C_p(T)$ and $\alpha(T)$ were made on the same C_{60} sample. Two series of $\alpha(T)$ measurement were made [14]. The results are illustrated in Fig. 6 (first — dashed line, second — solid line). The second series was made after series 1 and annealing the sample in vacuum (1 mTorr) at 450°C for 72 hours. It is seen that the temperature behavior of $C_p(T)$ and $\alpha(T)$ measured on the non-annealed and annealed samples is similar in interval from 5 to 20 K. In this temperature region the contribution of the orientational molecular vibrations (librations) to $C_{p,\text{lat}}(T)$ is dominant and
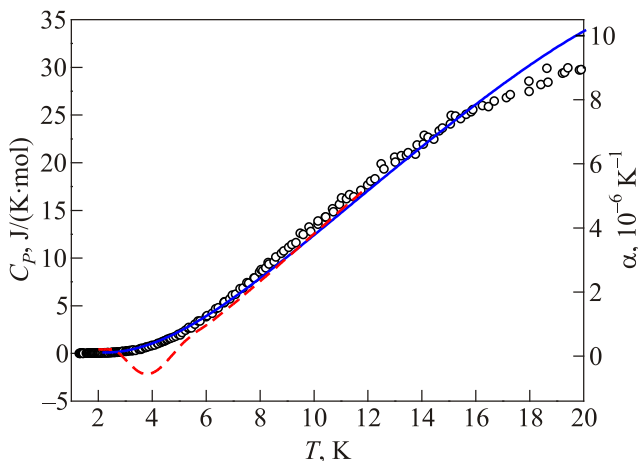
therefore $\alpha(T)$ is mainly determined by the anharmonicity of the orientational vibrations. Below 5 K the curves $C_p(T)$ and $\alpha(T)$ are close only for the annealed sample. The values of $\alpha(T)$ of the no annealed sample are negative at liquid helium temperatures. We attribute this to the influence of the impurities and defects present in the sample. The linear thermal expansion $\alpha(T)$ is very sensitive to these factors in C_{60} below 5 K [14].

The data on $\alpha(T)$ of a C_{60} single crystal [52] and $C_p(T)$ of our C_{60} powder sample are compare in the region from 5 to 120 K in Fig. 7. $\alpha(T)$ and $C_p(T)$ exhibit similar temperature dependences in the interval from 5 to 63 K. Above 60 K the curve $C_p(T)$ goes upwards due to the increasing contribution of the intramolecular vibrations (see Figs. 1(a), (b) and Fig. 2). The ratio $3\alpha/C_p$ determines the temperature dependence of the thermodynamic Grüneisen parameter

$$\gamma(T) = \frac{3\alpha}{C_V}\frac{V}{\chi_T},\qquad(2)$$

because the relation between the molar volume $V(T)$ and the isothermal compressibility $\chi_T(T)$ is only slightly temperature dependent at low temperatures. The correction $C_p - C_V$ is negligible at 60 K (0.2 J/(K·mol) [7]). As seen in Figs. 6 and 7, $\gamma(T)$ of fullerite C_{60} is only slightly dependent on temperature in the interval from 5 to 60 K. According to [53] $\gamma(T) \approx 3$. The behavior of $\alpha(T)$ and $\gamma(T)$ below 5 K is discussed in [14,48,49].

In the interval from 70 to 100 K the curve $\alpha(T)$ taken on a C_{60} single crystal [52] has a feature – a sharp rise and a jump of $\alpha(T)$ at $T_g \approx 86$ K (see Fig. 7). This feature of $\alpha(T)$ is also observed in x-ray and neutron diffraction studies (see Fig. 1 in [7]). Figure 7 suggests that the ratio α/C_p and hence $\gamma(T)$ have a jump in the region of the glass phase transition. Jumps of $\gamma(T)$ during orientational phase transitions ($T_g \approx 86$ K, $T_c \approx 260$ K) were observed in photoacoustic experiments [54]. The anomalous values of $\gamma(T)$ (and other physical properties) are essentially lower during the glass phase transition than in the case of an order-disorder phase transition.
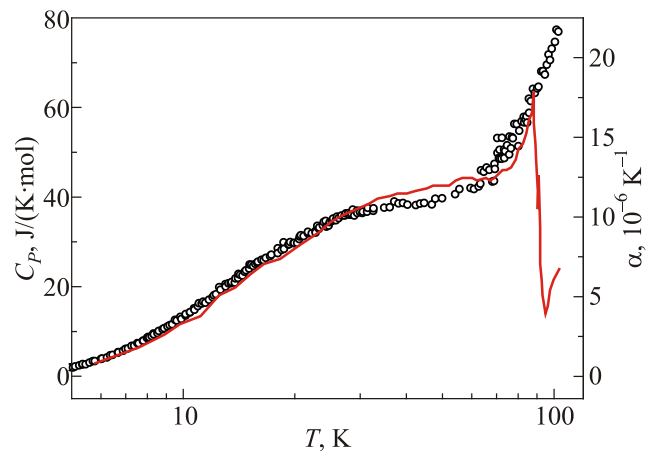

Fig. 6. (Color online) The comparison of the experimental curves $C_p(T)$ ((○) — our data) and the linear thermal expansion $\alpha(T)$ (dashed line — series 1, solid line — series 2) [14] of fullerite C_{60}.

Fig. 7. (Color online) The comparison of the experimental curves $C_p(T)$ ((○) — our data) and $\alpha(T)$ (solid line — [52]) of fullerite C_{60}.

Conclusion

The heat capacity of fullerite C_{60} at constant pressure has been investigated in the interval from 1.2 to 120 K using an adiabatic calorimeter. Our results and literature data were analyzed in the temperature interval from 0.2 to 300 K. The contributions of intramolecular and lattice vibrations to the heat capacity C_{60} have been separated. The contribution of intramolecular vibrations becomes essential above 50 K, being 50% at 100 K and over 90% above 270 K.

The contribution of acoustic modes to the heat capacity of C_{60} is dominant below 2.3 K. The Debye temperature at $T \to 0$ K has estimated ($\Theta_0 = 84.4$ K). The scatter of values of Θ_0 in literature data is caused mainly due from calculations involving the physical properties of C_{60} above 4 K as well as from the analysis procedures.

In the interval from 1.2 to 40 K the experimental curve of the heat capacity of the C_{60} lattice is caused the contributions of the rotational tunnel levels, translational vibrations (within the Debye model with $\Theta_0 = 84.4$ K) and librations (within the Einstein model with $\Theta_{E,\text{lib}} = 32.5$ K). $\Theta_{E,\text{lib}}$ agrees well with the libration maximum in the curve of the density of states estimated by the method of inelastic neutron scattering.

It is found that the experimental temperature dependences of heat capacity and thermal expansion are proportional in the region from 5 to 60 K. This suggests that the Grüneisen coefficient $\gamma(T)$ of fullerite C_{60} is only slightly dependent on temperature in this interval.

The features of the temperature dependences of the heat capacity of C_{60} in the regions of the heat capacity of C_{60} in the regions of the orientational glass T_g and order-disorder T_c phase transitions are determined by the potential field structure and the presence of p- and h-molecule configurations. In the orientationally ordered phase by the rotation of the molecules about the <111> axes the molecules can be in six potential wells with global and local minima, which correspond to the pentagonal (p) and hexagonal (h) configurations, respectively. The presence of a high (≈ 2900 K) barrier between the p- and h-configurations places the emphasis on the influence of the temperature prehistory on the physical properties of C_{60} crystals, which entails the hysteretic phenomena in the regions of phase transition.

In the high-temperature phase the specific heat of the lattice at constant volume is close to $4.5\,R$, which corresponds to the high-temperature limit for the translational lattice vibrations $(3\,R)$ and the near-free rotational motion of C_{60} molecules $(1.5\,R)$.

Acknowledgments

1. H.W. Kroto, J.R. Heath, S.C. O'Brien, R.F. Curl, and R.E. Smalley, *Nature* **318**, 162 (1985).
2. S. Rols, C. Bousige, J. Cambedouzou, P. Launois, J.-L. Sauvajol, H. Schober, V.N. Agafonov, V.A. Davydov, and J. Ollivier, *Eur. Phys. J. Special Topics* **213**, 77 (2012).
3. P.A. Heiney, G.B.M. Vaughan, J.E. Fisher, N. Coustel, D.E. Cox, J.R.D. Copley, D.A. Neumann, W.A. Kamitakahara, K.M. Creegan, D.M. Cox, J.P. McCauley, Jr., and A.B. Smith III, *Phys. Rev. B* **45**, 4544 (1992).
4. S.G. Stepanian, V.A. Karachevtsev, A.M. Plokhotnichenko, L. Adamowicz, and A.M. Rao, *J. Phys. Chem. B* **110**, 15769 (2006).
5. A.V. Peschanskii, A.Yu Glamazda, V.I. Fomin, and V.A. Karachevtsev, *Fiz. Nizk. Temp.* **38**, 1077 (2012) [*Low. Temp. Phys.* **38**, 854 (2012)].
6. L.S. Fomenko, V.D. Natsik, S.V. Lubenets, V.G. Lirtman, N.A. Aksenova, A.P. Isakina, A.I. Prokhvatilov, M.A. Strzhemechny, and R.S. Ruoff, *Fiz. Nizk. Temp.* **21**, 465 (1995) [*Low Temp. Phys.* **21**, 364 (1995)].
7. N.A. Aksenova, A.P. Isakina, A.I. Prokhvatilov, and M.A. Strzhemechny, *Fiz. Nizk. Temp.* **25**, 964 (1999) [*Low Temp. Phys.* **25**, 724 (1999)].
8. W.I.F. David, R.M. Ibberson, T.J.S. Dennis, J.P. Hare, and K. Prasside, *Europhys. Lett.* **18**, 219 (1992).
9. A.T. Pugachev, N.P. Churakova, N.I. Gorbenko, Kh. Saadli, and E.S. Syrkin, *Zh. Eksp. Teor. Fiz.* **114**, 1014 (1998).
10. A.T. Pugachev, N.P. Churakova, and N.I. Gorbenko, *Fiz. Nizk. Temp.* **23**, 854 (1997) [*Low Temp. Phys.* **23**, 642 (1997)].
11. R.D. Johnson, C.S. Yannoni, H.C. Dorn, J.R. Salem, and D.S. Bethune, *Science* **255**, 1235 (1992).
12. A.N. Aleksandrovskii, V.B. Esel'son, V.G. Manzhelii, B.G. Udovichenko, A.V. Soldatov, and B. Sundqvist, *Fiz. Nizk. Temp.* **23**, 1256 (1997) [*Low Temp. Phys.* **23**, 943 (1997)].
13. A.N. Aleksandrovskii, V.B. Esel'son, V.G. Manzhelii, B.G. Udovichenko, A.V. Soldatov, and B. Sundqvist, *Fiz. Nizk. Temp.* **26**, 100 (2000) [*Low Temp. Phys.* **26**, 75 (2000)].
14. A.N. Aleksandrovskii, A.S. Bakai, A.V. Dolbin, V.B. Esel'son, G.E. Gadd, V.G. Gavrilko, V.G. Manzhelii, S. Moricca, B. Sundqvist, and B.G. Udovidchenko, *Fiz. Nizk. Temp.* **29**, 432 (2003) [*Low Temp. Phys.* **29**, 324 (2003)].
15. A.N. Aleksandrovskii, A.S. Bakai, A.V. Dolbin, D. Cassidy, V.G. Manzhelii, and B. Sundqvist, *Fiz. Nizk. Temp.* **31**, 565 (2005) [*Low Temp. Phys.* **31**, 429 (2005)].
16. T. Atake, T. Tanaka, H. Kawaji, K. Kikuchi, K. Saito, S. Suzuki, I. Ikemoto, and Y. Ashiba, *Physica C* **185**–**189**, 427 (1991).
17. T. Atake, T. Tanaka, H. Kawaji, K. Kikuchi, K. Saito, S. Suzuki, Y. Ashiba, and I. Ikemoto, *Chem. Phys. Lett.* **196**, 321 (1992).
18. T. Matsuo, H. Suga, W.I.F. David, R.M. Ibberson, P. Bernier, A. Zahab, C. Farbe, A. Rassat, and A. Dworkin, *Solid State Commun.* **83**, 711 (1992).
19. B.V. Lebedev, K.B. Zhogova, T.A. Bykova, B.S. Kaverin, V.L. Karnatsevich, and M.A. Lopatin, *Rus. Chem. Bull.* **45**, 2113 (1996).

20. Y. Miyazaki, M. Sorai, R. Lin, A. Dworkin, H. Szwarc, and J. Godard, *Chem. Phys. Lett.* **305**, 293 (1999).

21. M.I. Bagatskii, V.V. Sumarokov, and A.V. Dolbin, *Fiz. Nizk. Temp.* **37**, 535 (2011) [*Low Temp. Phys.* **37**, 424 (2011)].

22. W.P. Beyermann, M.F. Hundley, J.D. Thompson, F.N. Diederich, and G. Grüner, *Phys. Rev. Lett.* **68**, 2046 (1992).

23. W.P. Beyermann, M.F. Hundley, J.D. Thompson, F.N. Diederich, and G. Grüner, *Phys. Rev. Lett.* **69**, 2737 (1992).

24. E. Grivei, M. Cassart, J.-P. Issi, L. Langer, B. Nysten, J.-P. Michenaud, C. Farbe, and A. Rassat, *Phys. Rev. B.* **44**, 8514 (1993).

25. J.R. Olson, K.A. Topp, and R.O. Pohl, *Science* **259**, 1145 (1993).

26. *Science of Fullerenes and Carbon Nanotubes,* M.S. Dresselhaus, G. Dresselhaus, and P.C. Eklund (eds.), Academic Press, San Diego (1996).

27. V.D. Natsik and A.V. Podolskiy, *Fiz. Nizk. Temp.* **26**, 304 (2000) [*Low Temp. Phys.* **26**, 225 (2000)].

28. E. Grivei, B. Nysten, M. Cassart, J-P. Issi, *C* Farbe, and A. Rassat, *Phys. Rev. B* **47**, 1705 (1993).

29. V.B. Efimov, L.P. Mezhov-Deglin, and R.K. Nikolaev, *Pis'ma Zh. Eksp. Teor. Fiz.* **65**, 651 (1997) [*JETP* **65**, 687 (1997)].

30. G. Pitsi, J. Caerels, and J. Thoen, *Phys. Rev. B* **55**, 915 (1997).

31. J.E. Fisher, A.R. McGhie, J.K. Estrada, M. Haluška, H. Kuzmany, and H.-U. ter Meer, *Phys. Rev. B* **53**, 11418 (1996).

32. N.M. Nemes, M. García-Hernández, G. Bortel, É. Kováts, B.J. Nagy, I. Jalsovszky, and S. Pekker, *J. Phys. Chem. B* **113**, 2042 (2009).

33. B. Sundqvist, *Physica B* **265**, 208 (1999).

34. S. Hoen, N.G. Chopra, X.-D. Xiang, R. Mostovoy, J. Hou, W.A. Vareka, and A. Zettl, *Phys. Rev.B* **46**, 12737 (1992).

35. L. Shebanovs, J. Maniks, and J. Kalnacs, *J. Cryst. Grow.* **234**, 202 (2002).

36. N.P. Kobelev, R.K. Nikolaev, Ya.M. Soĭfer, and S.S. Khasanov, *Fiz. Tverd. Tela* **40**, 173 (1998) [*Phys. Solid State* **40**, 154 (1998)].

37. V.P. Mikhal'chenko, *Fiz. Tverd. Tela* **52**, 1444 (2010) [*Phys. Solid State* **52**, 1549 (2010)].

38. *Theory of Anharmonic Effects in Crystals,* G. Leibfried and W. Ludwig (eds.), Academic Press Inc., New York-London (1961).

39. M.I. Bagatskii, V.V. Sumarokov, A.V. Dolbin, and S. Sundqvist, *Fiz. Nizk. Temp.* **38**, 87 (2012) [*Low Temp. Phys.* **38**, 67 (2012)].

40. M.I. Bagatskii, V.G. Manzhelii, V.V. Sumarokov, A.V. Dolbin, M.S. Barabashko, and B. Sundqvist, *Fiz. Nizk. Temp.* **40**, 873 (2014) [*Low Temp. Phys.* **40**, 678 (2014)].

41. A.M. Gurevich, A.V. Terekhov, D.S. Kondrashev, A.V. Dolbin, D. Cassidy, G.E. Gadd, S. Moricca, and B. Sundqvist, *Fiz. Nizk. Temp.* **32**, 1275 (2006) [*Low Temp. Phys.* **32**, 967 (2006)].

42. V. Schettino, M. Pagliai, L. Ciabini, and G. Cardini, *J. Phys. Chem. A* **105**, 11192 (2001).

43. K.A. Yagotintsev, M.A. Strzhemechny, Yu.E. Stetsenko, I.V. Legchenkova, and A.I. Prokhvatilov, *Physica B* **381**, 224 (2006).

44. M. Gu and T.B. Tang, *J. Appl. Phys.* **93**, 2486 (2003).

45. R.C. Yu, N. Tea, M.B. Salamon, D. Lorents, and R. Malhotra, *Phys. Rev. Lett.* **68**, 2050 (1992).

46. F. Negri, G. Orlandi, and F. Zerbetto, *Chem. Phys. Lett.* **144**, 31 (1988).

47. B. Tycko, R.C. Haddon, G. Dabbagh, S.H. Glarum, D.C. Douglass, and A.M. Mujsce. *J. Phys. Chem.* **95**, 518 (1991).

48. M.A. Ivanov and V.M. Loktev, *Fiz. Nizk. Temp.* **19**, 618 (1993) [*Low Temp. Phys.* **19**, 442 (1993)].

49. A.S. Bakai, *Fiz. Nizk. Temp.* **32**, 1143 (2006) [*Low Temp. Phys.* **32**, 868 (2006)].

50. M.I. Bagatskii, V.G. Manzhelii, M.A. lvanov, P.I. Muromtsev, and I.Ya. Minchina, *Fiz. Nizk. Temp.* **18**, 1142 (1992) [*Sov. J. Low Temp. Phys.* **18**, 801 (1992)].

51. V.G. Manzhellii, M.I. Bagatskii, I.Ya. Minchina, and A.N. Aleksandrovskii, *J. Low Temp. Phys* **111**, 257 (1998).

52. F. Gugenberger, R. Heid, C. Meingast, P. Adelmann, M. Braun, H. Wühl, M. Haluška, and H. Kuzmany, *Phys. Rev. Lett.* **69**, 3774(1992).

53. M.A. White, C. Meingast, W.I.F. David, and T. Matsuo, *Solid State Commun.* **94**, 481 (1995).

54. N.I. Odina and A.I. Korobov, *Fiz. Tverd. Tela* **56**, 811 (2014) [*Phys. Sol. State* **56**, 844 (2014)].